Viscoelastic Characterization of Polymers Using Instrumented Indentation. I. Quasi-Static Testing

M. R. VANLANDINGHAM,[1] N.-K. CHANG,[2] P. L. DRZAL,[1] C. C. WHITE,[1] S.-H. CHANG[2]

[1]National Institute of Standards and Technology, Gaithersburg, Maryland 20899-8615

[2]Department of Mechanical Engineering, National Taiwan University, Taipei, Taiwan

Received 4 October 2004; revised 12 January 2005; accepted 20 February 2005
DOI: 10.1002/polb.20454
Published online in Wiley InterScience (www.interscience.wiley.com).

ABSTRACT: The use of instrumented indentation to characterize the mechanical response of polymeric materials was studied. A model based on contact between a rigid probe and a linear viscoelastic material was used to calculate values for the creep compliance and stress relaxation modulus for two glassy polymeric materials, epoxy and poly(methyl methacrylate), and two poly(dimethyl siloxane) (PDMS) elastomers. Results from bulk rheometry studies were used for comparison with the indentation stress relaxation results. For the two glassy polymers, the use of sharp pyramidal tips produced responses that were considerably more compliant (less stiff) than the rheometry values. Additional study of the deformation remaining in epoxy after indentation creep testing as a function of the creep hold time revealed that a large portion of the creep displacement measured was due to postyield flow. Indentation creep measurements of the epoxy with a rounded conical tip also produced nonlinear responses, but the creep compliance values appeared to approach linear viscoelastic values with decreasing creep force. Responses measured for the unfilled PDMS were mainly linear elastic, with the filled PDMS exhibiting some time-dependent and slight nonlinear responses in both rheometry and indentation measurements. ©2005 Wiley Periodicals, Inc.* J Polym Sci Part B: Polym Phys 43: 1794–1811, 2005
Keywords: creep; indentation; modulus; relaxation; rheology; strain; stress; viscoelastic properties

INTRODUCTION

Instrumented indentation is increasingly being used to probe the mechanical response of polymeric and biological materials. These types of materials behave in a viscoelastic fashion, and thus their mechanical behavior is dependent on the test conditions, including the amount of strain, the strain rate, and the temperature. Often in instrumented indentation, however, properties are measured with loading histories and analysis developed for elastic and elastoplastic materials, for which time-dependent behavior is normally neglected. In studies in which attempts have been made to characterize viscoelastic behavior with indentation,[1,2] limiting and sometimes invalid assumptions have been made, and linear viscoelasticity has been applied despite the intense strains local to the indenter tip. Normally linear viscoelastic behav-

Certain commercial instruments and materials are identified in this article to adequately describe the experimental procedure. In no case does such identification imply recommendation or endorsement by the U.S. Army Research Laboratory or the National Institute of Standards and Technology, nor does it imply that the instruments or materials are necessarily the best available for the purpose.

Correspondence to: M. R. VanLandingham (E-mail: mvanlandingham@arl.army.mil)

Journal of Polymer Science: Part B: Polymer Physics, Vol. 43, 1794–1811 (2005)

ior is measured at small strain levels[3] in much the same way as an elastic modulus of a metal or ceramic would be measured at small strains at which linear elastic behavior dominates. However, unlike metals and ceramics, for which the elastic modulus can be estimated from indentation measurements with the unloading data, polymers exhibit viscoelastic behavior during indentation measurements such that similar calculations of the elastic modulus are inaccurate.

The mechanical response of viscoelastic materials is highly dependent on the types and levels of stress and strain as well as the strain rate. An analysis of indentation data, however, is typically based on force and displacement measurements, and stress and strain values are often estimated only in a nominal sense. For example, the mean stress, often used as a measure of the hardness, H, is the ratio of the force, P, to the contact area, A, where A is in general related to the displacement, h, by the tip geometry. Only in the case of a flat punch, for which A is constant with h, is H a function of force only. A general indentation strain rate can be calculated for any tip geometry from the ratio $\dot{h}/h$, where $\dot{h}$ is the rate of change of h with time t, or $\dot{h}$ is equal to dh/dt. For a paraboloidal tip, a representative measure of the indentation strain is proportional to the ratio of the contact radius, r, to the tip radius, R, where r is a function of h.[4–6] A nominal indentation strain for a conical or pyramidal tip is related to the characteristic included angle or angles of the tip and is not a function of h. For Vickers and Berkovich pyramidal indenters, which ideally have the same area function, $A(h)$, empirically based analyses attributed to Tabor[4] yield an estimated representative strain for these self-similar tips of 8–10%. However, Chaudhri[7] estimated that the representative strain ranged from 25 to 36% for a Vickers indentation of polycrystalline copper, and finite element analysis has been used to estimate strains local to a Berkovich indentation tip to be in excess of 100%, with a large volume of material subjected to at least 15% strain.[8] As discussed by Dao et al.,[8] values for a representative indentation strain will depend on the relationships between the indentation parameters and mechanical properties upon which its definition is based. Thus, for the indentation of polymeric materials, the representative strains may be different from that defined previously in other studies and may differ between different viscoelastic materials. Also, viscoelastic materials might be much more sensitive to the local variations in the strain and strain rate than metals and ceramics.

For polymeric and biological materials, a wide range of mechanical behavior can result from the imposition of finite strains. Analytical solutions of quasi-static contact between a rigid indenter and a linear viscoelastic solid[9–14] can be used to account for the viscoelastic constitutive behavior when indentation data are analyzed for these types of materials. These analyses are based on the development of an appropriate boundary-value problem that satisfies the equations of equilibrium. The stress–strain relations for linear, isotropic viscoelasticity are given by[12]

$$e_{ij}(t) = \frac{1}{2}\int_0^t J(t-\tau)\frac{\partial}{\partial\tau}s_{ij}(\tau)d\tau$$

$$s_{ij}(t) = 2\int_0^t G(t-\tau)\frac{\partial}{\partial\tau}e_{ij}(\tau)d\tau \qquad (1)$$

$$\varepsilon_{ij}(t) = \frac{1}{3}\int_0^t B(t-\tau)\frac{\partial}{\partial\tau}\sigma_{ij}(\tau)d\tau$$

$$\sigma_{ij}(t) = 3\int_0^t K(t-\tau)\frac{\partial}{\partial\tau}\varepsilon_{ij}(\tau)d\tau \qquad (2)$$

$B(t)$ and $K(t)$ are the dilatational creep and relaxation functions, respectively, relating the stress and strain invariants, σ_{ii} and ε_{ii}, τ is a "dummy" variable for time in the integral notation, and t is time. $J(t)$ and $G(t)$ are the shear creep and relaxation functions, respectively, relating the deviatoric stress tensor, s_{ij}, and the deviatoric strain tensor, e_{ij}.

These expressions are formulated in terms of integral operators associated with the hereditary function, so that relaxation times are given by a continuous spectrum. Alternatively, these expressions can be restated in terms of differential operators with a viscoelastic model of springs and dashpots, corresponding to a discrete spectrum of relaxation times, or with other equivalent ways of expressing linear viscoelastic behavior, including direct measurements.[9,10,12] The following single-integral constitutive equation has also been used:[11,13]

$$\sigma_{ij} = \left[\int_{0^-}^{t} 2G(t-\tau)\frac{\partial \varepsilon_{ij}(\tau)}{\partial \tau} + \delta_{ij}\lambda(t-\tau)\frac{\partial \varepsilon_{kk}(\tau)}{\partial \tau}\right] d\tau \tag{3}$$

$G(t)$ is again the relaxation modulus in shear, and Lamé's constant, $\lambda(t)$, is related to the relaxation modulus in extension, $E(t)$, and Poisson's ratio, $v(t)$. The lower limit of 0^- is used in case of a jump in stresses and strains at $t = 0$. For homogeneous, isotropic, elastic materials, E, G, and v are related by

$$G = \frac{E}{2(1+v)} \tag{4}$$

This equation holds for a viscoelastic solid only at equilibrium. Also, for viscoelastic materials, the shear, bulk, and extensional creep compliances, $J(t)$, $B(t)$, and $D(t)$, respectively, are not simple inverse functions of their respective relaxation moduli, $G(t)$, $K(t)$, and $E(t)$, as they are for elastic materials, and v is, in general, a function of time,[3] although it is often taken to be constant for simplicity. Finally, creep compliance is generally determined as the ratio of an applied constant stress, σ_0, and the resulting time-dependent strain, $\varepsilon(t)$, and the stress relaxation modulus is normally determined as the ratio of an applied constant strain, ε_0, and the resulting time-dependent stress, $\sigma(t)$, in both cases under uniaxial loading conditions.

Viscoelastic solutions to boundary value problems can often be solved by the application of the Laplace transform to remove the variable, t, from the system of equations. This approach yields an elastic problem in the transformed variables. With the elastic solution to the transformed problem, a viscoelastic solution is achieved by the replacement of the elastic constants with the appropriate viscoelastic operators; that is, the elastic–viscoelastic correspondence principle is invoked, and then the inverse Laplace transform is performed. In the case of the given contact problem, however, the boundary conditions are normally taken from the compatibility between displacements and stresses with the prescribed surface displacements and surface tractions, respectively, and these conditions are a function of time.[9–11] Therefore, in general, the transform approach is not applicable, although a solution by Lee and Radok[10] of this type for an incompressible material ($v = 0.5$) has been shown to be valid for a monotonically increasing contact radius. A slightly different approach by Ting[11] yields separate solutions for increasing and decreasing contact radius.

Indentation analogues to creep and relaxation measurements have been suggested. For indentation creep, a constant force P_0 is applied at $t = 0$ and held. During such a test, the penetration depth, $h(t)$, and hence the contact area, $A(t) = \pi r^2(t)$, increase with time such that the stress is not constant but rather decreases with time. Additionally, the stress state below the indenter tip will be multiaxial rather than uniaxial. Despite these departures from traditional creep testing, viscoelastic contact models have been applied to the indention creep problem to yield the following relationship between $J(t)$, P_0, $A(t)$, and $h(t)$ for a paraboloidal indenter of radius R:

$$J(t) = \frac{8h(t)\sqrt{A(t)}}{3\sqrt{\pi}(1-v)P_0} \tag{5}$$

Simplifications related to eq 5 include the assumptions that v is constant and that $J(t)$ is equal to $1/G(t)$. The indentation analogue to stress relaxation involves conditions in which a constant penetration depth, h_0 (with a corresponding contact area, A_0), is applied at $t = 0$ and held. Although the state of stress is again complex, the nominal indentation strain should remain relatively constant. For a paraboloidal indenter of radius R, viscoelastic contact models give the following relationship between $G(t)$, h_0, A_0, and the force, $P(t)$:

$$G(t) = \frac{3\sqrt{\pi}(1-v)P(t)}{8h_0\sqrt{A_0}} \tag{6}$$

Again, v is assumed to be constant. Additionally, the Ting model yields equations for constant-force indentation creep and constant-depth stress relaxation for conical tips:

$$J(t) = \frac{A(t)}{(1-v)P_0 \tan\theta} \tag{7}$$

$$G(t) = \frac{(1-v)P(t)\tan\theta}{A_0} \tag{8}$$

In these equations, θ is the cone semiapical angle, and v is assumed constant in both equations. The additional assumption that $J(t)$ is equal to $1/G(t)$ is made in eq 7. Also, eqs 7 and 8 were recently derived for pyramidal indenters[6] directly from Hooke's law under the assumption

that a representative stress is given by P/A and a representative strain is given by $(\cot\theta)(dh/h)$. Thus, the creep compliance and relaxation modulus in eqs 5–8 appear to be ratios of these simple representations for stress and strain. In indentation analysis, pyramidal tips are often modeled as perfect conical tips, often with an additional geometric factor that is related to noncircular contact areas of pyramidal tips with respect to conical tips.[8] Although eqs 7 and 8 were applied to pyramidal tip indentation measurements in this study, this additional geometric factor, normally a 3–5% correction of the contact area, was not used.

In recent efforts to measure the viscoelastic behavior of polymers with instrumented indentation, linear viscoelastic models, including models similar to the Ting model and the Lee–Radok model and/or simple spring–dashpot models (e.g., the standard linear solid), have been applied.[1,2,6,15,16] Whether or not linear viscoelasticity is obeyed during instrumented indentation measurements, however, is difficult to ascertain. The intense stresses and strains expected local to the tip–sample contact as well as the mixed stress conditions suggest that simple linear viscoelastic relations may not be applicable. One test of linear viscoelasticity is the lack of dependence of the creep compliance (or stress relaxation modulus) on the magnitude of the stress (or strain). Although this condition is necessary but not sufficient proof of linear viscoelasticity, eqs 5–8 present an opportunity to determine for paraboloidal and conical (and presumably pyramidal) indentation probes if linear viscoelasticity is not obeyed under particular test conditions. Additionally, these equations provide a means of measuring viscoelastic behavior with instrumented indentation that can be compared to other types of rheological measurements.

In this article, analyses based on contact between a rigid indenter and a linear viscoelastic material are used to calculate $J(t)$ and $G(t)$ from instrumented indentation testing. Four different polymers are characterized with traditional rheometry and with measurements of the constant-force indentation creep and constant-depth stress relaxation. For the indentation measurements, checks of linear viscoelasticity are performed by the study of the dependence of the creep compliance on the indentation force. The resulting measurements of the creep compliance and relaxation modulus are compared with traditional rheometry measurements.

EXPERIMENTAL

Materials

The materials used in this study included an amine-cured epoxy, poly(methyl methacrylate) (PMMA), and two poly(dimethyl siloxane) (PDMS) materials. Epoxy films approximately 190 μm thick were cast onto silicon wafers in a CO_2-free and H_2O-free glovebox with a drawdown technique. Highly pure diglycidyl ether of bisphenol A with a mass per epoxy equivalent of 172 g (DER 332, Dow Chemical) and 1,3-bis(aminomethyl)cyclohexane (Aldrich) were mixed at the stoichiometric ratio. All samples were cured at room temperature for 48 h, and this was followed by postcuring at 130 °C for 2 h. The films were then removed from the silicon substrates by immersion in warm water and then peeling with tweezers. The PMMA sample was obtained from a commercial Plexiglas acrylic sheet from AtoHaas North America, Inc. The PDMS samples were obtained from Dow Corning Corp. The first sample (called filled PDMS) was a general-purpose (GP-50) silica-filled crosslinked PDMS with a thickness of 3.2 mm. The second, unfilled PDMS sample was made from Sylgard 184 mixed at a 10:1 (resin/crosslinker) ratio. This PDMS material was cast onto a glass plate, degassed for 30 min at 20 inHg, and cured for 4 h at 65 °C; this resulted in a sample thickness of 2.7 mm. The glass-transition temperature (T_g) for epoxy and PMMA was estimated with differential scanning calorimetry with heating and cooling rates of 10 °C/min; the values were determined from cooling. The values of T_g for the PDMS materials were determined as the peak in the loss modulus with shear rheometry with a heating rate of 2 °C/min, 0.05% strain, and a frequency of 1 Hz. The resulting values of T_g were 112 ± 1 °C for the epoxy films, 106 ± 1 °C for PMMA, −67 ± 3 °C for the filled PDMS, and −120 ± 2 °C for the unfilled PDMS. Because all other rheological testing was performed at room temperature, the values for Poisson's ratio were assumed to be 0.3 for the epoxy and PMMA samples and 0.5 for the PDMS samples. For each material studied, rheometry testing and indentation testing were performed concurrently over a span of approximately 3 days, and so physical aging times for the epoxy and PMMA were assumed to be the same for all tests.

Solid Rheometry Measurements

Stress relaxation measurements were made in torsion on the filled PDMS material with an advanced rheometric expansion system (ARES, Rheometrics Scientific, Inc.) and in tension on the PMMA and epoxy samples with a rheological solids analyzer (RSA II, Rheometrics Scientific, Inc.). The unfilled PDMS material was tested in compression with the RSA II. Instrumental capabilities limited the amount of strain applied to PDMS samples in the ARES to 0.08 (8%) and in the RSA II to 0.01 (1%). Equation 4 was used to convert measurements of the stress relaxation modulus in tension or compression, $E(t)$, to that in shear, $G(t)$.

Instrumented Indentation Measurements

Instrumented indentation was performed with a NanoIndenter XP and a NanoIndenter DCM (MTS Systems, Inc.). The XP system, in general, was used for applied forces from 100 to 0.2 mN, whereas the DCM system was used for applied forces from 10 to 0.01 mN. Both systems could be used to characterize the epoxy and PMMA samples, but only the DCM system could be used to characterize the much more compliant PDMS samples because of the force resolution limitations of the XP system. For measurements made with the XP system, two different probe tip shapes were used, a Berkovich pyramidal tip and a rounded 90° conical tip with a tip radius of approximately 10 μm (manufacturer specification). Only a Berkovich tip was available for testing with the DCM system. The tip shape has been measured for these probes by the indentation of reference samples and by the direct imaging of the probes with an atomic force microscope, as detailed elsewhere.[17] For the indentation creep and stress relaxation tests, a technique often called the continuous stiffness method was employed, in which a small harmonic oscillation was superposed over the constant force (creep) or displacement (relaxation) with a frequency of 45 Hz and an amplitude of approximately 5 nm, as controlled with signal feedback. An appropriate dynamic model of the system[18] with an assumption of negligible damping was then used to calculate values of A as a function of h for use in eq 5–8.

The indentation creep response was measured with step loading to a prescribed force, P_0, which was then held for 100 s. For a given test, P_0 was reached in less than 0.1 s and was maintained within ± 2 μN for the XP system and ± 1 μN for the DCM system. After this near-step loading, however, the harmonic oscillation superposed over the constant force required time to stabilize before measurements of the contact area were considered to be accurate. This time lapse was approximately 10–12 s for the XP system and 4–5 s for the DCM system. To monitor the thermal drift rate of the system, the same constant force test method was performed on fused silica before and after each set of tests on a polymer sample. Because the system thermal drift could be positive or negative, no attempt was made to remove the system drift from the creep measurements. Rather, the hold time was limited to approxi-

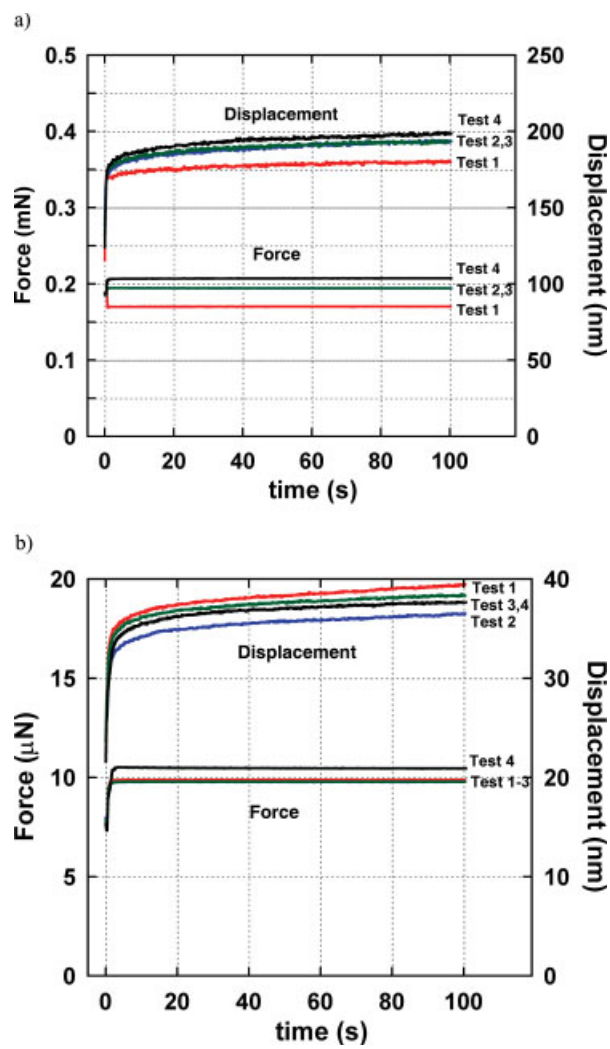

Figure 1. Examples of system performance for the indentation creep tests for (a) the XP system with a 200 μN force and (b) the DCM system with a 10 μN force. Both examples are for a Berkovich tip indenting epoxy. [Color figure can be viewed in the online issue, which is available at www.interscience.wiley.com]

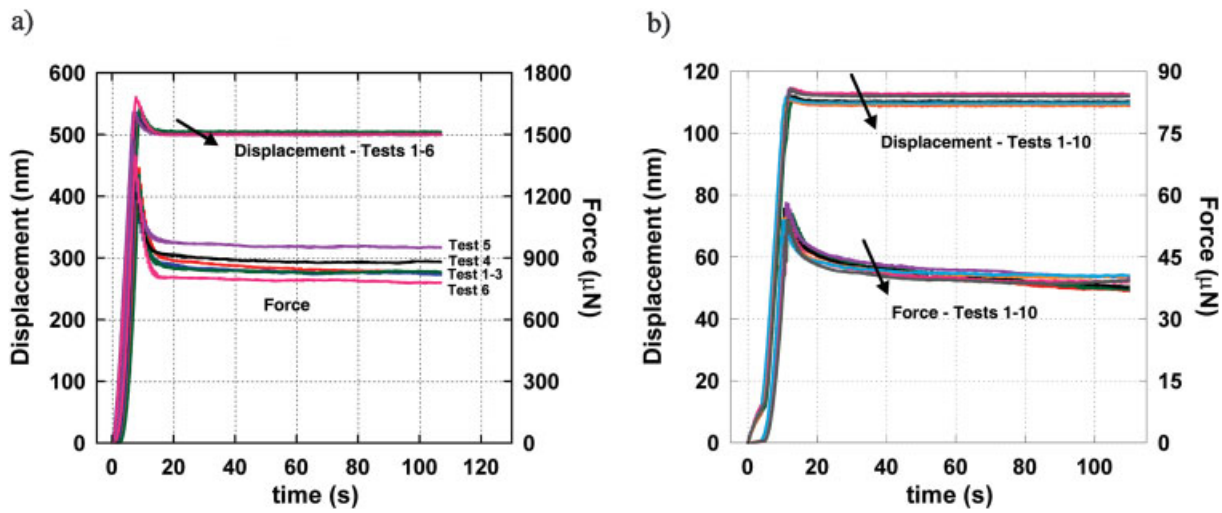

Figure 2. Examples of system performance for the indentation stress relaxation tests for (a) the XP system with a 500 nm displacement and (b) the DCM system with a 100 nm displacement. Both examples are for a Berkovich tip indenting epoxy.

mately 100 s, at which point the creep rates for the two glassy polymers became of the same order as the drift rate (ca. ± 0.02 nm/s). For a set of four or more tests at the same nominal force, the difference between the lowest and highest values of P_0 was less than 50 μN for the XP system and 3 μN for the DCM system, regardless of the magnitude of the prescribed force. Examples of system performance at the lowest applied creep forces are shown in Figure 1(a) for the XP system and in Figure 1(b) for the DCM system. Creep compliance was calculated with eq 5 or 7 according to the tip geometry.

The indentation relaxation response was measured with a step displacement to a prescribed depth, h_0. As for the indentation creep tests, the length of the relaxation tests was limited to 100 s to minimize uncertainty due to system thermal drift. For a given test, h_0 was reached in approximately 6 s, and this was followed by a period of roughly 6–8 s during which the system feedback attempted to control the displacement at the prescribed constant value. A slight overshoot of approximately 5–10% of h_0 was observed for the XP system, and an overshoot of 1–3% of h_0 was observed for the DCM

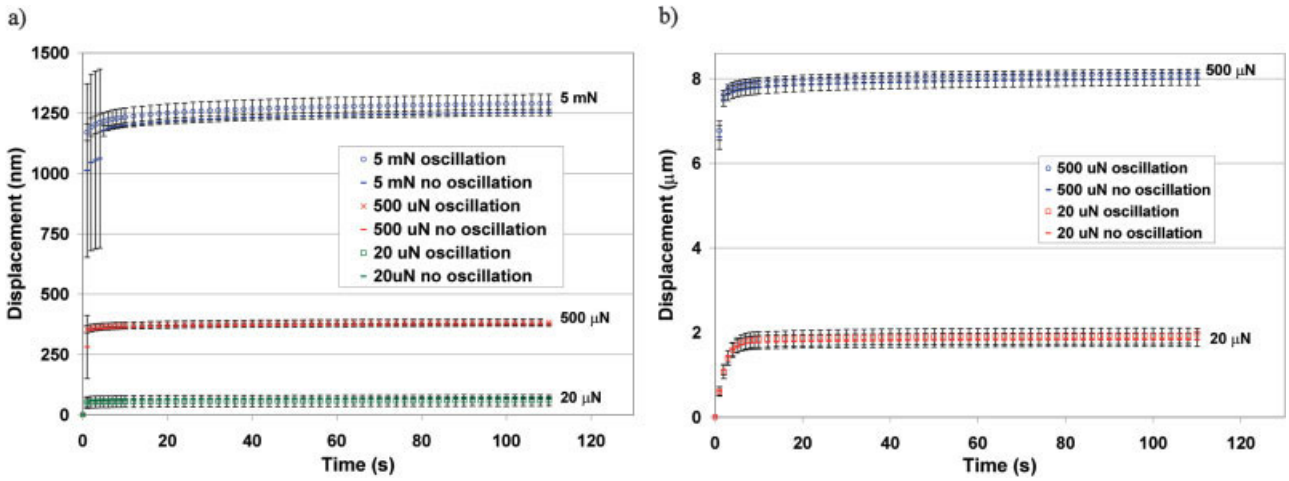

Figure 3. Displacement plotted as a function of time for indentation creep tests with and without a superposed 5 nm amplitude dynamic oscillation at 45 Hz for several quasi-static creep force levels: (a) epoxy and (b) PDMS. All data are for the DCM system and a Berkovich tip.

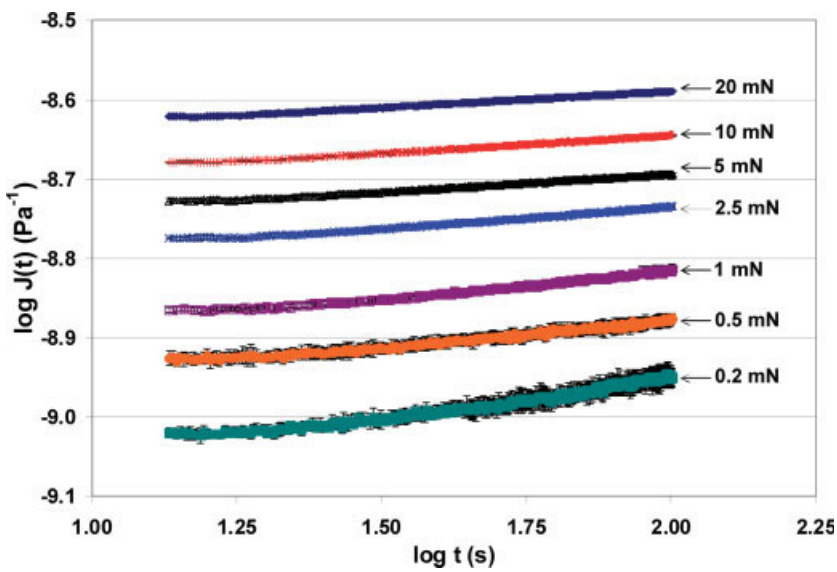

Figure 4. Log–log plot of the creep compliance, $J(t)$, for an indentation creep experiment on epoxy with a rounded conical tip (manufacturer-determined tip radius of 10 μm) and the XP system. Each data point represents an average value from a minimum of eight experiments (two to three sets of four to six tests), with the error bars representing an estimated standard deviation ($k = 1$). In some cases, the error bars are smaller than the data point symbols. [Color figure can be viewed in the online issue, which is available at www.interscience.wiley.com]

system. After the initial overshoot, displacement was maintained within ±1–2 nm for both the XP and DCM systems, except for very large displacements with the XP system, for which displacement variations were as much as ±5 nm for a nominal displacement of 4000 nm. For a set of 10 tests at the same nominal depth, the difference between the lowest and highest values of h_0 was less than 5 nm for both systems for target depths of 1500 nm or less and 10 nm for target depths greater than 1500 nm. However, the repeatability of the force values was better for the DCM system than for the XP system. Examples of system performance at the lowest applied depth levels are shown in Figure 2(a) for the XP system and in Figure 2(b) for the DCM system. The relaxation modulus was calculated with eq 6 or 8 according to the tip geometry.

Residual Depth (RD) Measurements

An additional study of RD as a function of time for indentation creep measurements on epoxy was made for a Berkovich tip and the DCM system. The same type of indentation creep test described in the previous subsection was used. However, the creep force was removed after 20 s for five tests, after 50 s for five tests, and after 100 s for five tests for each of three force levels: 0.05, 0.5, and 5 mN. The samples were stored in a laboratory environment overnight and then scanned in the tapping mode with a Digital Instruments Dimension 3100 atomic force microscope and a NanoScope 3a controller (Veeco Metrology). One image of each residual impression was captured, and cross-section and bearing analyses provided in the offline atomic force microscopy (AFM) software were used to determine the depth of the impression.

RESULTS AND DISCUSSION

Effect of Harmonic Oscillation

As detailed in the Experimental section, a harmonic oscillation was superposed over the quasi-static forces in the indentation creep and stress relaxation measurements; a controlled displacement amplitude of approximately 5 nm and a frequency of 45 Hz was used for both the XP and DCM systems. Although the harmonic displacement was generally small with respect to the quasi-static displacements, the dissipated energy could have caused an increase in the temperature that would have altered the measured response in comparison with tests made without this harmonic oscillation. In Figure 3,

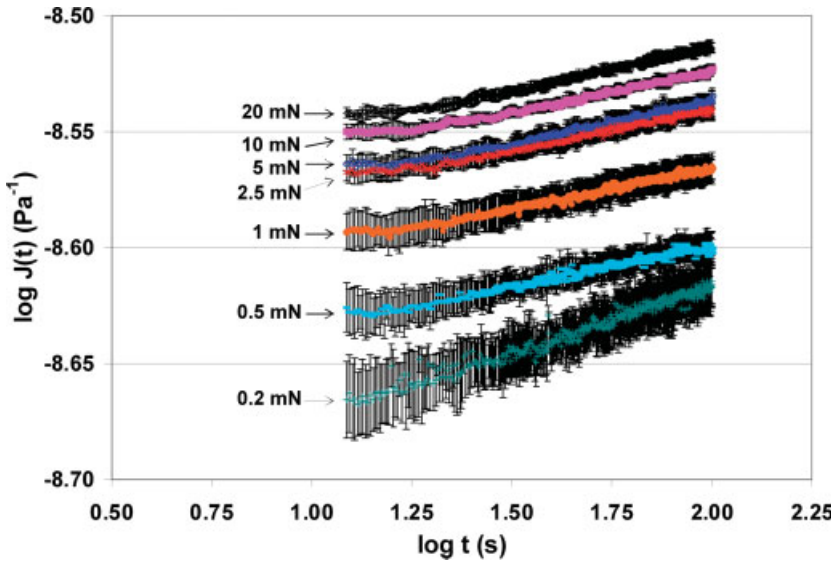

Figure 5. Log–log plot of the creep compliance, $J(t)$, for an indentation creep experiment on epoxy with a Berkovich tip and the XP system. Each data point represents an average value from a minimum of eight experiments (two to three sets of four to six tests), with the error bars representing an estimated standard deviation ($k = 1$). [Color figure can be viewed in the online issue, which is available at www.interscience.wiley.com]

the displacement responses to several creep forces are shown as a function of time for both the epoxy and filled PDMS. In both cases, the evolution of the displacement with time was identical within the experimental uncertainty for the measurements made with and without the harmonic oscillation component.

Creep and Stress Relaxation of Epoxy and PMMA

An example of indentation creep compliance determined for an epoxy sample with a rounded conical tip (manufacturer-determined tip radius of 10 μm) is shown in Figure 4. The creep compliance is clearly dependent on the indentation

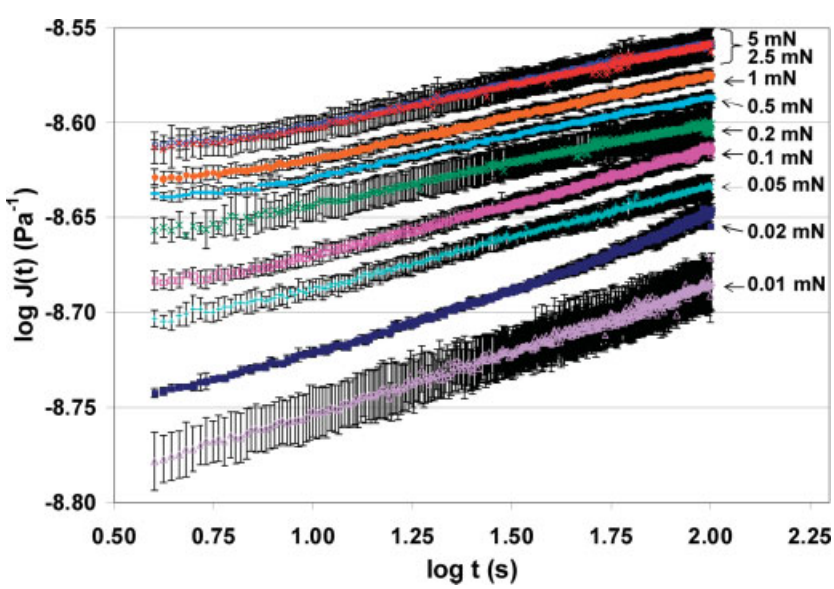

Figure 6. Log–log plot of the creep compliance, $J(t)$, for an indentation creep experiment on epoxy with a Berkovich tip and the DCM system. Each data point represents an average value from a minimum of eight experiments (two to three sets of four to six tests), with the error bars representing an estimated standard deviation ($k = 1$). [Color figure can be viewed in the online issue, which is available at www.interscience.wiley.com]

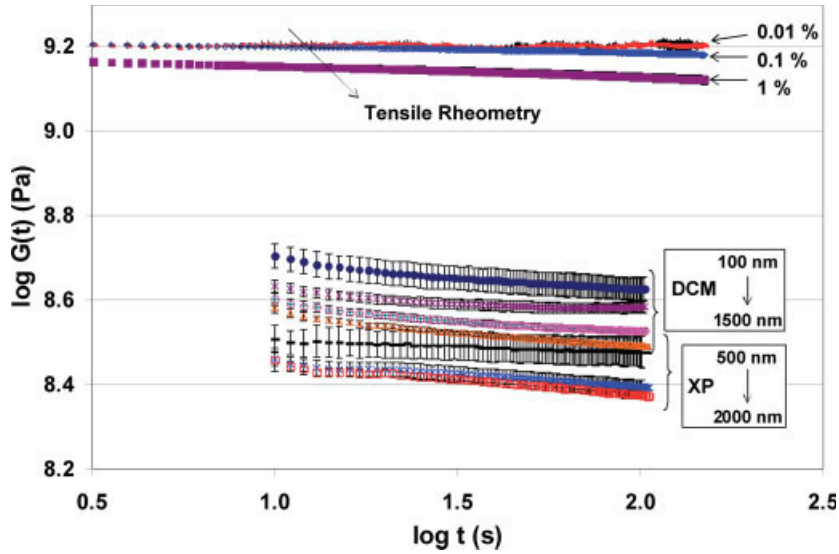

Figure 7. Log–log plot of the stress relaxation modulus, $G(t)$, for an indentation relaxation experiment on epoxy with a Berkovich tip and both the XP and DCM systems. Each data point represents an average value from a minimum of eight experiments (two to three sets of four to six tests). Superposed on the plot are rheometry results from the RSA II system in tension [$G(t)$ was converted from $E(t)$ with eq 4], for which each data point represents an average of three experiments. For all data shown, the error bars represent an estimated standard deviation ($k = 1$). The percentages for the tensile rheometry data represent the percentage of the strain applied to the samples. [Color figure can be viewed in the online issue, which is available at www.interscience.wiley.com]

forces between 0.2 and 20 mN, and this is an indication of nonlinear behavior. The creep compliance was also observed to be a function of force for the epoxy sample with Berkovich indentation tips for both the XP (Fig. 5) and the DCM (Fig. 6). Furthermore, the compliance values for the two sets of Berkovich indentation tests were similar for similar applied force levels, with differences likely due to slight differences in the tip geometry[17] leading to differences in the applied stress field.

Qualitatively, the data appear to be consistent with the behavior expected of a glassy epoxy polymer:[3,19] compliance values are on the order of 10^{-9} Pa and trend higher with increasing creep time and increasing force. Additionally, the trends in the compliance values with time appear to be similar for each of the force levels studied with the rounded cone and for the higher force levels with the Berkovich tips, and this suggests separability of the time-dependent behavior from the stress-dependent behavior.[3] The differences in the slope at the lower indentation creep forces for the Berkovich tips (Figs. 5 and 6) could have resulted from uncertainties in the tip shape related to indentation depths less than 100 nm. Normally, the tip shape is determined for a large range of contact depths, and the curve fits used to represent the area function tend to match the tip shape data best at larger depths at which the pyramidal angle dominates. The error percentage in the contact area at shallow depths was estimated to be at most 10%, which would shift the $J(t)$ data up by less than 0.05 log units.

The results of stress relaxation testing are presented for epoxy in Figure 7, including Berkovich tip indentation and rheometry data. For the data measured with the RSA II rheometer in tension on the epoxy material, the stress relaxation modulus values were similar for strain levels of 0.01 and 0.1%. The application of a 1% strain, however, resulted in lower modulus values and a slight increase in the time dependence in comparison with the two lower strain levels; this is typical of nonlinear viscoelastic behavior of glassy polymers.[3] Similar behavior was observed for the stress relaxation modulus values measured with indentation with a Berkovich tip: increases in the applied constant displacement resulted in lower relaxation modulus values. Although relatively small for a glassy polymer at room temperature, the time dependence measured with indentation was similar to that measured with rheometry.

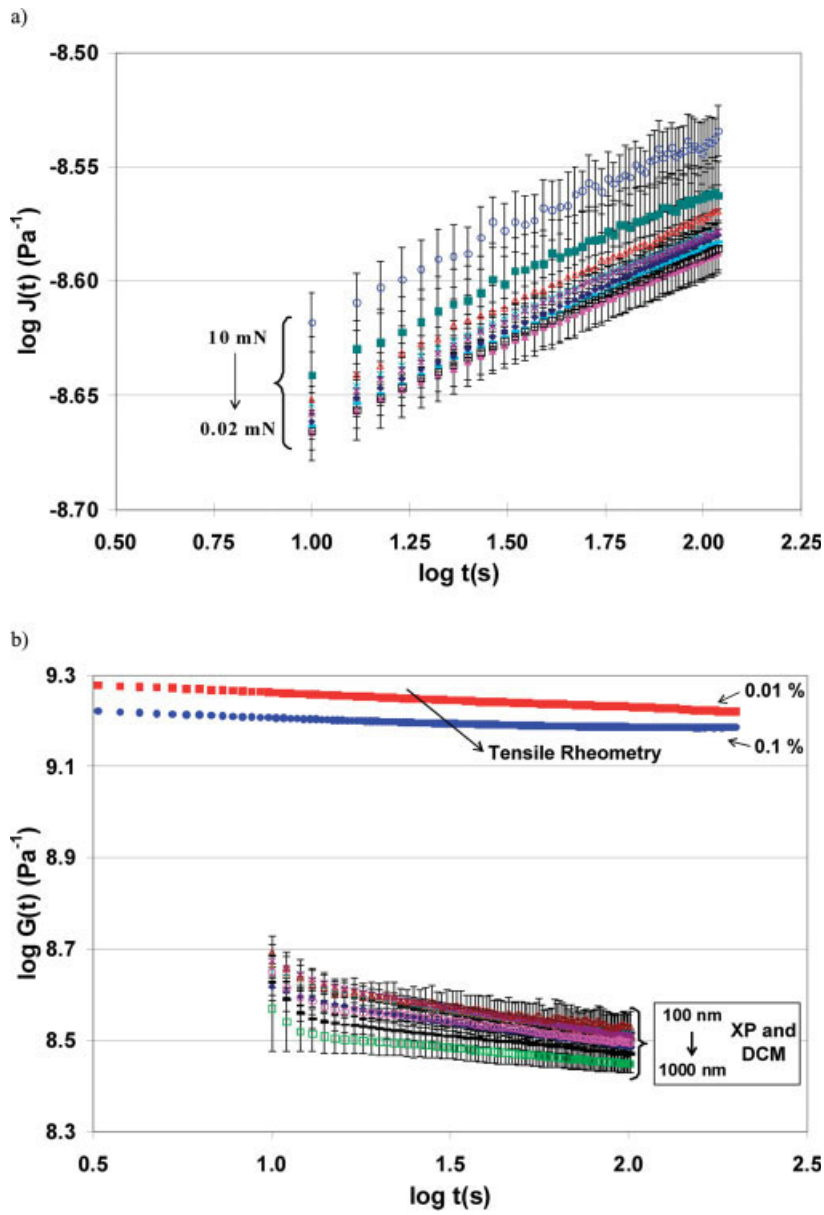

Figure 8. Log–log plots of (a) the creep compliance, $J(t)$, and (b) the stress relaxation modulus, $G(t)$, for indentation creep and stress relaxation experiments, respectively, on PMMA with a Berkovich tip and both the XP and DCM systems. Each data point represents an average value from a minimum of eight experiments (two to three sets of four to six tests), with the error bars representing an estimated standard deviation ($k = 1$). Superposed on part b are rheometry results from the RSA II system in tension [$G(t)$ was converted from $E(t)$ with eq 4], for which each data point represents an average of three experiments. For all data shown, the error bars represent an estimated standard deviation ($k = 1$). The percentages for the tensile rheometry data represent the percentage of the strain applied to the samples. [Color figure can be viewed in the online issue, which is available at www.interscience.wiley.com]

In Figure 8, log–log plots of the creep compliance and stress relaxation modulus are shown for PMMA. The indentation data in these plots were collected with Berkovich tips with both the XP and DCM systems. The data are again qualitatively consistent with behavior expected of a glassy polymer, and the magnitudes of the creep compliance and relaxation modulus values are

very similar to values determined for epoxy (see Figs. 5–7). However, the indentation values appear to be less dependent on the indentation force (creep) or indentation displacement (relaxation). This observation seems to indicate less strain sensitivity for PMMA than for epoxy at the large strain levels imposed during Berkovich tip indentation.

Comparing the Berkovich tip indentation measurements of $J(t)$ and $G(t)$ for epoxy and PMMA (see Figs. 5–8), we found that an increase in the applied force caused $J(t)$ to increase, and an increase in the displacement caused a decrease in $G(t)$; this is consistent with the qualitatively reciprocal nature of these functions. Furthermore, the assumption that $J(t)G(t)$ is equal to 1 appears to hold for tests in which the force and displacement levels were similar. For example, with the DCM data from Figures 6 and 7, respectively, J(2.5 mN, 10 s) was 1.74×10^{-9} Pa^{-1} and G(1000 nm, 10 s) was 0.56×10^{9} Pa; therefore, $J(t)G(t)$ was 0.97. However, the values of $G(t)$ measured via indentation with a Berkovich tip were much lower than the $G(t)$ values calculated from tensile rheometry, by 70–80% for epoxy and by 80% for PMMA. For many polymers, the stress relaxation modulus decreases significantly with increasing strain, and so the trends with time are similar and the data can be superposed by vertical shifts.[3] Thus, this discrepancy could be related to the much larger strain levels related to indentation tests with a Berkovich tip in comparison with the rheometry tests.

To explore whether the measured creep response was mainly viscoelastic or included a significant contribution from yield behavior, the residual indentation depth was studied for the Berkovich indentation of epoxy with the DCM system; the results are shown in Figure 9. The differences between the measured creep displacement, h, and the corresponding RD values measured with AFM are shown for different creep hold periods. For example, h(100 s) – h(20 s) represents the difference in the creep displacement measured for a hold time of 100 s and that measured for a hold time of 20 s, as measured with the DCM system; the corresponding difference in RD between an impression produced for a hold time of 100 s and that produced for a hold time of 20 s is designated RD(100 s) – RD(20 s). Examples of RD measurements with AFM are shown in Figure 9(b,c) for a 5 mN creep force and hold times of 20 s and 100 s, respectively. On the basis of the vertical distance measurements shown, the corresponding RD values were RD(20 s) = 304.2 nm and RD(100 s) = 337.9 nm. After the averaging of five such measurements for each creep force and hold time, the average values were subtracted to yield the data in Figure 9(a). For each of the three force levels, the increase in h with time is associated with a significant increase in RD. Thus, for the Berkovich indentation of epoxy, the measured change in the creep displacement over a give period appears to largely consist of material flow characteristic of yield or postyield conditions rather than a purely viscoelastic creep response, even at very low force levels (50 μN). The corresponding measurements of $J(t)$ and $G(t)$ thus contain a substantial contribution from yield phenomena, and this explains the large differences in comparison with the values associated with viscoelastic behavior. This conclusion likely also applies for the Berkovich indentation of PMMA and the indentation results for epoxy with the rounded conical tip.

To estimate the levels of strain applied during the indentation measurements, effective strains were calculated for the Berkovich and rounded conical tip shapes used with the XP system. These calculations were made with empirically based analyses attributed to Tabor[4] in which ideal plastic behavior was assumed. Although the postyield flow significantly affected the measured indentation response for epoxy and PMMA, these materials are far from ideal plastic materials. Thus, this analysis is at best qualitative. The following two equations were used to estimate the effective strain, $\bar{\varepsilon}$, for ideal paraboloidal and conical tip geometries, respectively:

$$\bar{\varepsilon} = 0.2r/R \tag{9}$$

$$\bar{\varepsilon} = 0.25 \cot \theta \tag{10}$$

For the Berkovich tip, an effective conical angle, θ, was determined to be approximately 70.45°. For the rounded cone, an effective radius, R_{eff}, was determined from tip shape analysis to range from 4 μm at shallow depths to 10 μm at larger depths.[17] In Figure 10, data from Figures 4 and 5 are combined to show that the corresponding $J(t)$ values are lower for the rounded conical tip, except for 10 and 20 mN. Additionally, the $J(t)$ values for the rounded conical tip at 2.5 and 5 mN creep forces are similar to values for the Berkovich tip and the DCM system at the lower creep force levels (see Fig. 6). The relative effec-

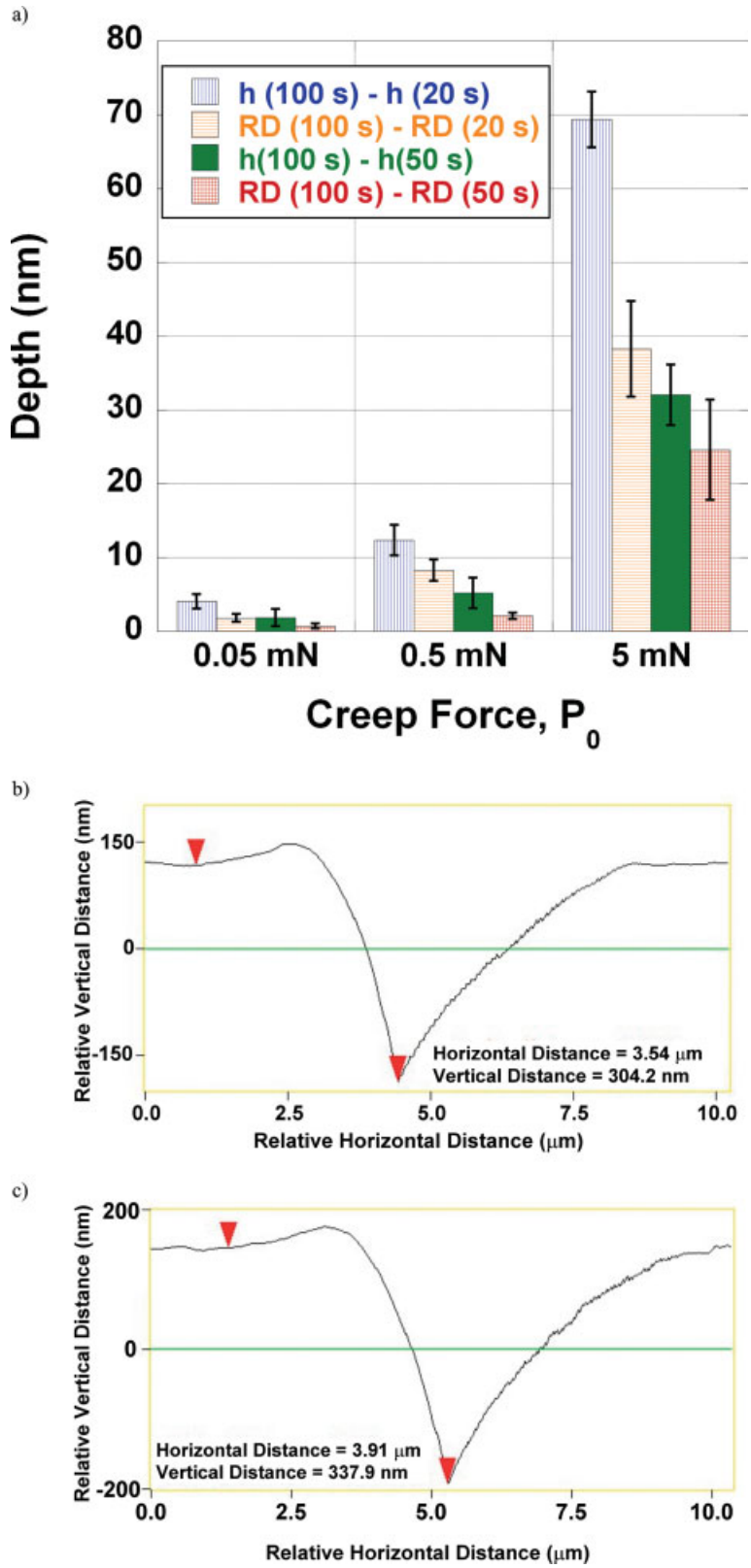

Figure 9. (a) Bar chart representing the differences between the measured creep displacement, h, for the Berkovich indentation of epoxy with the DCM system and the corresponding RD values measured with AFM. Each data point represents an average of five experiments, and the error bars represent the corresponding estimated standard deviation ($k = 1$). (b,c) Examples of cross sections from AFM images for a 5 mN creep force after 20 and 100 s hold periods, respectively. [Color figure can be viewed in the online issue, which is available at www.interscience.wiley.com]

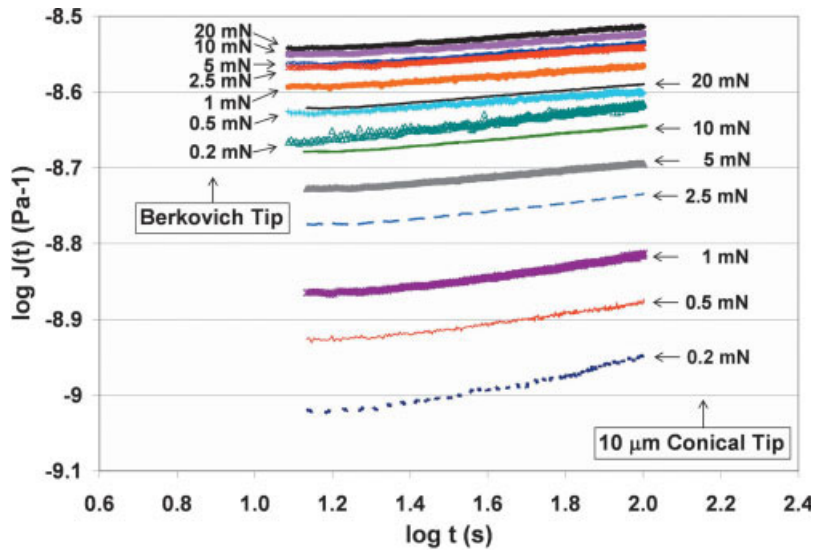

Figure 10. Log–log plot of the creep compliance, $J(t)$, as a function of time t, comparing the indentation creep data for epoxy from Figures 4 (rounded conical tip and XP) and 5 (Berkovich tip and XP). The error bars were removed for clarity. [Color figure can be viewed in the online issue, which is available at www.interscience.wiley.com]

tive strain, shown in Figure 11, is also similar for the rounded conical tip in comparison with a Berkovich tip for creep forces of 2.5 mN and higher. Thus, at these higher creep forces, the effective strains and the corresponding $J(t)$ values for the rounded conical tip are similar to those for the Berkovich tips. Also, the larger variation in the creep compliance for the rounded conical tip with force reflects the larger expected changes in the associated effective strain in comparison with the Berkovich tip. Although the plots in Figure 11 indicate no expected variation in strain imposed by an ideal Berkovich tip, a small variation in the effective strain related to deviations in the actual tip geometry from the ideal case could have affected the measurements. More likely, however, the epoxy is sensitive not only to the nominal strain level, such as that based on eq 10, but also to local strain levels that perhaps are mildly dependent on displacement.

In Figure 11(b), a snapshot of $J(t)$ at $t = 50$ s for epoxy is shown as a function of the estimated effective strain for the rounded conical tip (from Fig. 4) and the Berkovich tip (from Fig. 5) used with the XP system. The dashed line represents a linear extrapolation of the strain dependence of $J(t = 50$ s) to small strains for the rounded conical tip data. This extrapolation appears to indicate that, at strain levels below 1%, $J(t)$ values should approach values typically measured for epoxy under conditions of linear viscoelastic behavior. Thus, achieving such small strain values for indentation measurements will likely require the use of large rounded tips and small penetration depths to reduce the r/R ratio to appropriate levels.

PDMS Creep and Stress Relaxation

Indentation creep compliance results for the filled PDMS material with a Berkovich tip and the DCM system are shown in Figure 12. Again, the data appear, at least qualitatively, to be consistent with the expected behavior:[3] the compliance values are on the order of 10^{-6} Pa and trend slightly higher with increasing creep time. Also, the compliance values generally tend to decrease with increasing force. However, the data scatter was significant, and, for much of the force range, that is, between 100 μN and 2 mN, $J(t)$ appears to be similar.

The results of stress relaxation testing are presented for both PDMS materials in Figure 13, including indentation and rheometry data. Nonlinear behavior was observed for the filled PDMS in the rheometry measurements in torsion, as $G(t)$ values decreased with increasing strain levels. A small amount of time dependence, which decreased with increasing strain, was also observed. In comparison, the relaxation behavior of the unfilled PDMS [Fig. 13(b)] meas-

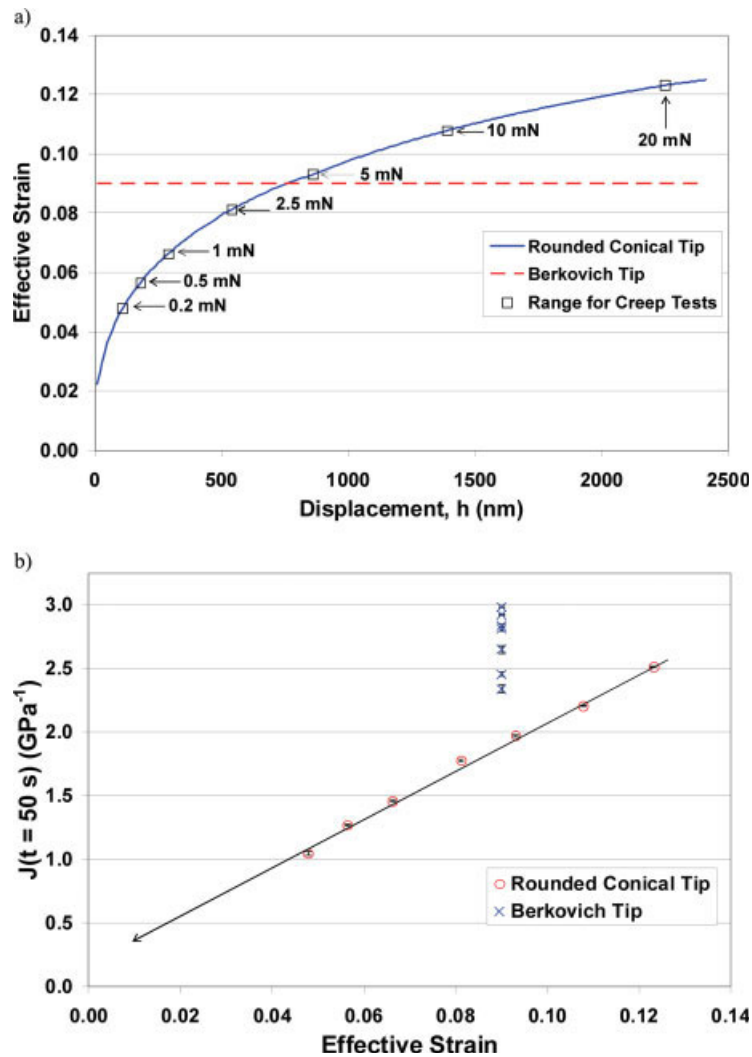

Figure 11. (a) Plot of the effective strain estimates (after Tabor;[4] predictions of the effective strain, $\bar{\varepsilon}$, were made with eqs 9 and 10 with tip shape information) measured for the Berkovich and rounded conical tips used in this study and (b) plot of the creep compliance, $J(t)$, at time $t = 50$ s for epoxy as a function of the estimated effective strain for the rounded conical tip and the Berkovich tip used with the XP system. The dashed line represents a linear extrapolation of the strain dependence of $J(t = 50$ s) to small strains. [Color figure can be viewed in the online issue, which is available at www.interscience.wiley.com]

ured in compression was linear elastic; although the rheometry data is shown only for a strain of 0.05%, the response measured over a range of strain levels (data not shown) was the same within the experimental uncertainty as that shown. Both the nonlinear response at relatively low strain levels and the slight time dependence observed in Figure 13(a) are probably related to the presence of the silica filler. Unfilled PDMS is linear elastic to large strain levels, whereas lightly filled PDMS and other rubbery cross-linked polymers often behave in a nonlinear elastic fashion, sometimes with a slight time dependence; this is consistent with the observed behavior.

For the filled PDMS, the indentation relaxation modulus values were independent of the penetration depth for depths from 1 to 5 μm within the data scatter. For penetration depths of 10 and 15 μm, the relaxation modulus values are again similar to but slightly higher than those for the three smaller penetration depths.

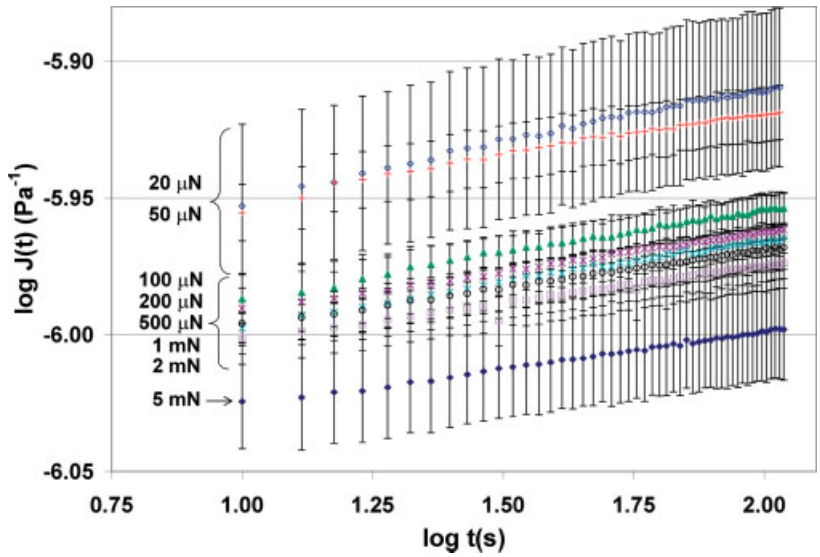

Figure 12. Log–log plot of the creep compliance, $J(t)$, for an indentation creep experiment on PDMS with a Berkovich tip and the DCM system. Each data point represents an average value from a minimum of eight experiments (two to three sets of four to six tests), with the error bars representing an estimated standard deviation ($k = 1$). [Color figure can be viewed in the online issue, which is available at www.interscience.wiley.com]

Similarly for the unfilled PDMS, the indentation relaxation modulus values were independent of the penetration depth for depths from 3.5 to 20 μm within the data scatter, with values corresponding to depths of 2.5 and 0.75 μm being slightly lower. The correspondence of larger values of $G(t)$ to larger penetration depths could be related to several factors. First, this trend could be the result of a stiffening effect due to a restriction of network motion with increased local strain levels. Second, the tip shape was characterized only for contact depths less than 500 nm because of the maximum force limitations of the DCM system when fused silica glass is indented. The curve fit to this tip shape data was then extrapolated to the much larger contact depths reached during the indentation of PDMS samples, and thus the error in the values of the area used in the calculations likely increased with increasing contact depth. Additionally, because the PDMS materials are extremely compliant, the identification of the initial point of tip–sample contact is difficult. In fact, penetration depths of hundreds of nanometers or more can occur at force levels on the order of 1 μN, largely because of the competing tip–sample adhesion forces. This problem of detecting initial contact combined with the limited tip shape information available could have caused the trend in $G(t)$ values with depth, as uncertainties in the initial contact point will have a larger influence on data taken at smaller depths. Until these measurement issues are solved, understanding whether such measured trends are real or artificial will be difficult.

The difference in the PDMS relaxation modulus values between the rheometry measurements and indentation measurements is large for both PDMS materials. Comparing $G(t)$ values from torsion measurements at 8% strain with the indentation $G(t)$ values for the filled PDMS, we found that both sets of data exhibited a similar lack of time dependence, but the indentation values were lower by 65%. The difference in the indentation values in comparison with the rheometry values at 1% strain increased to 70%. For the unfilled PDMS, the difference was even larger, ranging from 85% for the larger penetration depths to 95% for a depth of 0.75 μm. The larger difference for the unfilled PDMS with respect to the filled PDMS could be related to the larger influence of uncertainties related to detecting the initial contact point and the larger influence of tip–sample adhesion on the contact mechanics for the more compliant unfilled material.

For the stress relaxation modulus data for epoxy, PMMA and PDMS [Figs. 7, 8(b), and 13, respectively], any potential vertical shifting of the curves as a function of the strain level

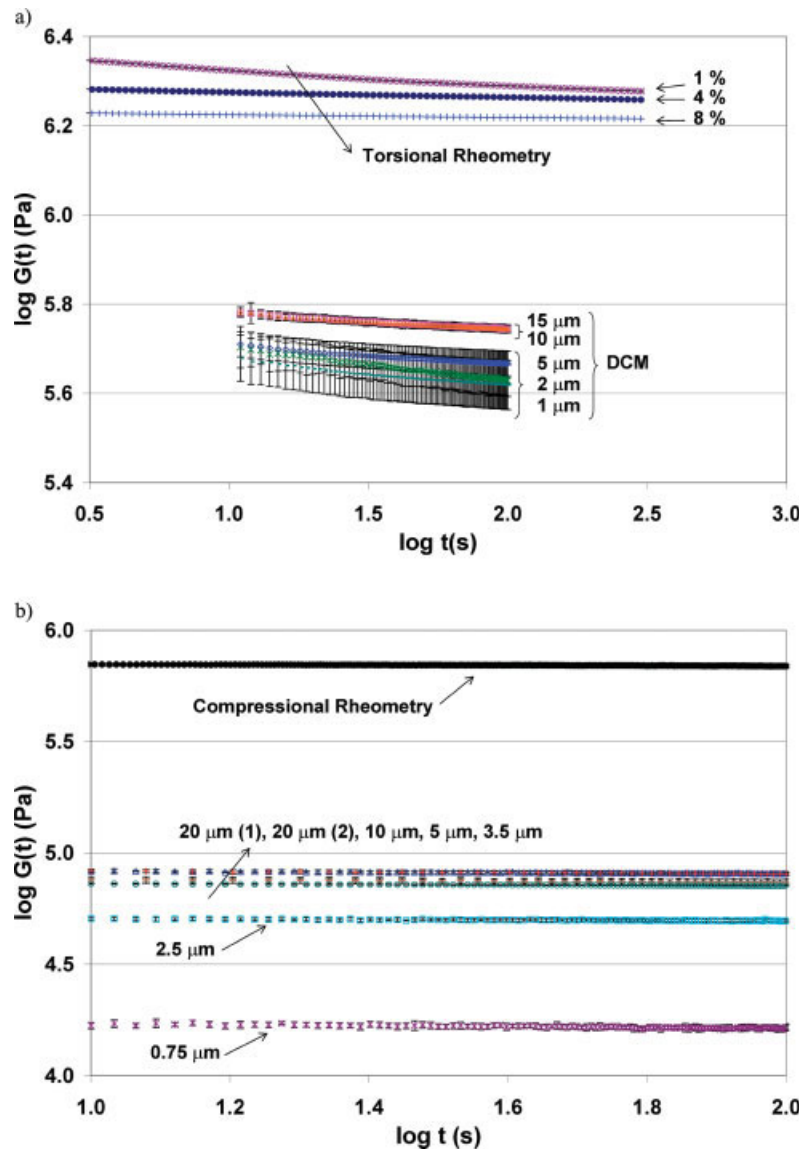

Figure 13. Log–log plots of the stress relaxation modulus, $G(t)$, for relaxation experiments on the two PDMS materials: (a) filled PDMS and (b) unfilled PDMS. Indentation relaxation measurements were made with a Berkovich tip and the DCM system. Each data point represents an average value from a minimum of eight experiments (two to three sets of four to six tests). Superposed on the plots are rheometry results. In part a, data are shown for the ARES torsional rheometer; in part b, data from the RSA II in compression are shown [$G(t)$ was converted from $E(t)$ with eq 4]. For all rheometry data shown, each data point represents an average of three experiments, and the error bars represent an estimated standard deviation ($k = 1$). The percentages given in part a for the torsional rheometry data represent the percentage of the strain applied to the samples. [Color figure can be viewed in the online issue, which is available at www.interscience.wiley.com]

would tend to indicate much larger effective strains in the indentation measurements with respect to the rheological measurements. However, a number of complicating factors exist regarding the indentation creep and stress relaxation measurements. First, for Berkovich indentation and likely for indentation with the rounded conical tip, the strain levels were large enough to induce yielding of the epoxy and PMMA, potentially causing the much lower

relaxation modulus values and much higher creep compliance values with respect to traditional viscoelastic measurements. For the PDMS materials, uncertainties associated with a lack of tip shape information at large depths, problems detecting the point of initial tip–sample contact, and tip–sample adhesion also present problems regarding the quantitative nature of the indentation measurements. Second, the calculations of the indentation creep compliance and stress relaxation modulus were based on a linear viscoelastic model, whereas the measurements indicated nonlinear viscoelastic and yield behavior for the epoxy and PMMA and nonlinear elastic behavior for the filled PDMS. Also, the model does not include effects of tip–sample adhesion, which likely played a significant role in the PDMS measurements. Finally, the measurements of $J(t)$ and $G(t)$ were based on a dynamic model of the indentation system in which damping at the tip–sample junction is assumed to be negligible; this assumption was potentially violated in these measurements. Thus, the absolute magnitudes of the indentation values of $J(t)$ and $G(t)$ plotted in Figures 4–10, 12, and 13 are not without significant uncertainty. However, the exhibited behavior appears to be consistent with rheometry measurements and with the known bulk rheology of these polymers at the high stress and strain levels expected under the indenter tip.

CONCLUSIONS

The use of instrumented indentation to characterize the mechanical response of polymeric materials was studied. A model based on contact between a rigid probe and a linear viscoelastic material was used to calculate values for the creep compliance and stress relaxation modulus for epoxy, PMMA, and two PDMS materials. Bulk rheometry studies were used for comparison. Unfortunately, the magnitudes of the indentation and rheometric values of the creep compliance or stress relaxation modulus are difficult to compare directly. This deficiency is related to the following factors:

1. The indentation values were calculated with an analytical model based on linear viscoelastic behavior that does not include tip–sample adhesion. However, the majority of the measured responses were nonlinear, particular for the Berkovich tip indentation of glassy epoxy and PMMA samples, for which a significant fraction of the response was due to yield behavior. Also, tip–sample adhesion likely affected the results for the PDMS materials.
2. For compliant materials, such as PDMS, detecting the point of initial tip–sample contact is challenging and can lead to artificial trends in modulus and compliance values. Additionally, the large penetration depths that must be used to overcome low force limitations of the instrumented indentation system require large extrapolations of tip geometry data that can lead to errors in the magnitudes of the modulus and compliance.
3. Although the use of harmonic oscillation superposed over the quasi-static forces did not alter the measured creep and stress relaxation responses, the determination of the contact area, which was used to calculate the creep compliance and relaxation modulus, was based on a dynamic model of the indentation system in which damping at the tip–sample junction is assumed to be negligible. For viscoelastic materials, this assumption might be violated, and in fact, a separate assumption of infinite load-frame stiffness can be used to extract energy storage and loss characteristics of polymers.
4. Often in the analysis of instrumented indentation data, factors are applied to correct for differences in experimental contact conditions and model contact conditions. However, these correction factors, which were not used in this study, have been determined for linear elastic and elastoplastic constitutive behavior, and the appropriateness of their use for viscoelastic behavior is unknown.

Despite these issues, the trends in the indentation data are similar to those in the rheometry data, and this suggests that the measurements may, in certain cases, have sufficient physical similarity. However, care must be taken to understand the behaviors being measured with respect to the stress and strain levels applied under the indentation tip. With such understanding, the large magnitude and nonuniformity of the strains and the mixed deformation modes associated with indentation measurements can be used potentially to access a wide

range of viscoelastic behavior by variations of the tip shape and force (depth) levels. This capability would include the potential to use large rounded tips to measure linear viscoelastic characteristics, with the understanding that tip–sample adhesion plays a more prominent role as the tip size increases. New analyses and measurement protocols are currently being explored for developing a more complete understanding of the relationships between instrumented indentation data and viscoelastic behavior.

The authors gratefully acknowledge fruitful collaborations with John Villarrubia of the National Institute of Standards and Technology regarding tip shape determination with atomic force microscopy, Sheng Lin-Gibson of the National Institute of Standards and Technology regarding torsional rheometry measurements, Xiaohong Gu of the National Institute of Standards and Technology for epoxy sample preparation, and Vincent Jardret, formerly of MTS Systems Corp., for his help with the test method development. The authors also acknowledge helpful discussions with Don Hunston of the National Institute of Standards and Technology and Greg McKenna of Texas Tech University.

REFERENCES AND NOTES

1. Cheng, L.; Xia, X.; Yu, W.; Scriven, L. E.; Gerberich, W. W. J Polym Sci Part B: Polym Phys 2000, 38, 10.
2. Yoder, K. B.; Ahuja, S.; Dihn, K. T.; Crowson, D. A.; Corcoran, S. G.; Cheng, L.; Gerberich, W. W. Fundamentals of Nanoindentation and Nanotribology 522; Materials Research Society: Pittsburgh, PA, 1998; p 205.
3. Ferry, J. D. Viscoelastic Properties of Polymers; Wiley: New York, 1980.
4. Tabor, D. Hardness of Metals; Clarendon: Oxford, 1951.
5. Briscoe, B. J.; Fiori, L.; Pelillo, E. J Phys D: Appl Phys 1998, 31, 2395.
6. Shimizu, S.; Yanagimoto, T.; Sakai, M. J Mater Res 1999, 14, 4075.
7. Chaudhri, M. M. Acta Mater 1998, 46, 3047.
8. Dao, M.; Chollacoop, N.; Van Vliet, K. J.; Venkatesh, T. A.; Suresh, S. Acta Mater 2001, 49, 3899.
9. Lee, E. H. Q. Appl Math 1955, 13, 183.
10. Lee, E. H.; Radok, J. R. M. J Appl Mech 1960, 27, 438.
11. Ting, T. C. T. J Appl Mech 1966, 33, 845.
12. Yang, W. H. J Appl Mech 1966, 33, 395.
13. Hunter, S. C. J Mech Phys Solids 1960, 8, 219.
14. Graham, G. A. C. Int J Eng Sci 1965, 3, 27.
15. Lu, H.; Wang, B.; Ma, J.; Huang, G.; Viswanathan, H. Mech Time-Dependent Mater 2003, 7, 189.
16. Oyen, M. L.; Cook, R. F. J Mater Res 2003, 18, 139.
17. Juliano, T. F.; Hagon, M. J. Meas Sci Technol, accepted for publication, 2005.
18. Lucas, B. N.; Oliver, W. C.; Swindeman, J. E. Fundamentals of Nanoindentation and Nanotribology 522; Materials Research Society: Pittsburgh, PA, 1998; p 3.
19. Lee, A.; McKenna, G. B. Polymer 1990, 31, 423–430.